AN EXPERIMENTAL STUDY OF ENERGY ABSORPTION CAPACITY
OF
HIGH-STRENGTH STEEL BEAMS

by

Toshiro SUZUKI[1] and Tetsuro ONO[2]

SUMMARY

The objectives of this paper are to understand the plastic behavior of high strength steel beams, especially the relations between local buckling, lateral buckling, accumulated strain and torsional deflection, and to determine quantitatively the energy absorption capacity and the total deflected value, comparing withthe resultes of low-alloy steel members. By evaluating with absolute values, the accumulated energy absorption capacities that are nondimensionalized with the ratio of yield stress to maximum stress take the same value, in spite of kinds of steel materials and repeated amplitutes. This result shows that the evaluation of energy absorption capacity by the absolute value becomes one evaluated method considering the deformation capacity of high-strength steel members for the aseismic design.

1. INTRODUCTION

As large sized steel structures have been developed, the high-strength steels having high yield stress level have attracted special interests recently. This study attemptes to correlate the plastic behavior and plastic deformation capacity of high-strength steel beams subjected to repeated bending with their material properties. It has been conventional practice to evaluate the deformation capacity of structural members by the ratio of the amount of post-yield deformation to the amount of elastic deformation from the viewpoint of plastic design. It is, however, questionable whether this evaluation method can be successfully applied to high-strength steels that sustain higher yield stresses but have less ductility than low-carbon steels. The present study has subjected beam members, including high-strength steels, to repeated bending. This paper discusses the effects of cumulative local strain and torsional deformation on the deterioration of the hysteresis loop, and reevaluates the deformation capacity of high-strength steels from the standpoint of aseismic design of structres by paying particular attention to the energy absorption capacity of the steel

---

1. Professor, Tokyo Institute of Technology, JAPAN
2. Associate Professor, Nagoya Institute of Technology, JAPAN

2. OUTLINE OF TESTS

Test specimens are built-up H section members (H-250 x 125 x 12 x 12), and the test steels are SM-41, SM-50, HT-60 and HT-80. These material properties are shown in Table 1. The moment distribution is under uniform moment (type A) and under moment gradient (type B). The slenderness ratio of beams, λ_y, is approximately 50 under uniform moment (type A) and 76 under moment gradient (type B). The test specimens are 21 in total and are outlined in Table 2. The experimental loading conditions are shown in Fig. 1 and Photo. 1.

Each test beam is loaded by controlling its central displacement. The fundamental repeated displacements are shown in Figs. 2 and 3. Type A beams under uniform moment are subjected to repeated loading with both constant and random displacement amplitudes, while type B beams under moment gradient are subjected to repeated loading with constant displacement amplitude alone. On repeated loading with random displacement amplitude, the amplitude of first loop is maximum value and 2nd through 5th loop are minimum amplitute and displacement beyond 6th loop is intermediate value.

3. EXPERIMENTAL HYSTERESIS LOOP AND ACCUMULATED STRAIN

Figs. 4 through 6 show the load-deformation relationships of HT-60 beams repeatedly loaded by varying the displacement amplitude. Each displacement amplitude is based on the displacement ($V/V_p = 2.0$) at the point of maximum load under monotonic loading. $V/V_p = 2.0$ (A-60-1), 2.5 (A-60-2), and 3.0 (A-60-3). The greater displacement amplitude, the more pronounced the deterioration of the hysteresis loop.

Figs. 7 and 8 show changes in the axial strain and torsional deformation of the central cross section of beam A-60-1. The strain decreases as the hysteresis loop deteriorates and indicates that there is little or no axial strain accumulation. It is clearly shown, on the other hand, that the torsional deformation is accumulated as the hysteresis loop deteriorates.

Figs. 9 and 10 show the amounts of axial strain (ε_i) and torsional deformation (β_i) accumulated in each test specimen, when the energy absorption capacity of the hysteresis loop has deteriorated to two-thirds of that of the virgin hysteresis loop. ε_1 and β_1 are strain and torsional angle of the virgin loop. This result indicates that the accumulation of axial strain is pronounced for high-strength steel beams and that the accumulation of torsional deformation is pronounced for low-carbon steel beams. This finding corresponds

232

to the fact that the prevailing type of deformation at the
time of bearing strength drop is local buckling deformation
for the high-strength steel beams and lateral buckling defor-
mation for the low-carbon steel beams.

4. ENERGY ABSORPTION CAPACITY OF
STEEL MEMBERS

Figs. 11 and 12 give the relationships between the energy
absorption capacity (E_{1j}) in each of the experimentally
obtained hysteresis loops and the cumulative energy absorption
capacity (ΣE_{1j}) in terms of nondimensional quantity of
energy under full plastic load. Whether the moment distribu-
tion is under uniform moment or under moment gradient, the
results expressed in nondimensional quantities show that the
energy absorption capacity is far higher with the low-carbon
steel beams than with the high-strength steel beams and de-
creases with an increase in tensile strength. There is found
such a tendency that the energy absorption capacity of each
grade of steel converges to a certain constant level, irre-
spective of displacement amplitude.

Figs. 13 and 14 show the energy absorption capacity in
dimensional, absolute quantities. When compared in absolute
quantities, the differences among the test steels in energy
absorption capacity decreases, and the steel grades are revers-
ed in the magnitude of thier energy absorption capacity with
the high-strength steels showing higher energy absorption
capacities. The limit to which the energy absorption capacity
ultimately converges is, however, at the same level, in-
dependent of the steel type.

Fig. 15 shows in absolute quantities the energy absorp-
tion capacity of type A beams subjected to repeated loading
with random displacement amplitude. Fine lines in the diagram
indicate the results of repeated loading at constant displace-
ment amplitude. The process of energy absorption under re-
peated loading with random displacement amplitude corresponds
to that under repeated loading at constant displacement ampli-
tude of the same magnitude. This means that the hysteresis
process of repeated loading with random displacement amplitude
can be inferred from the experimental results of repeated
loading at constant displacement amplitude.

Fig. 16 shows the relationships between the displacement
amplitude and cumulative energy absorption capacity in both
nondimensional and absolute quantities. The cumulative energy
absorption capacity are sum total until the energy absorption
capacity of the hysteresis loop has deleriorated to one half
of that of the virgin loop. Open circles denote nondimensional
quantities, and solid circles denote absolute quantities.

The cumulative energy absorption capacity is different with different steel grades when evaluated by the nondimensional quantity, but is the same, regardless of the steel grade, when evaluated by the absolute quantity. For the same grade of steel, the smaller the displacement amplitude, the greater the cumulative energy absorption capacity.

Assuming that the beam reaches its service limit when the energy absorption capacity of the hysteresis loop deteriorates to one half of that of the virgin hysteresis loop, Fig. 17 shows the product of the absolute quantity of energy absorped by each steel up to that time and its ratio of yield stress to maximum stress, k, in relation to its yield stress. Under monotonic loading, the amount of cumulative energy absorption multiplied by the ratio of yield stress to maximum stress is the same for all of the tested steels. A virtually similar tendency also holds under repeated loading, although there is some difference depending on the moment distribution.

5. CONCLUSION

The following can be concluded from the above.

When evaluated by its absolute quantity, the energy absorption capacity of each steel converges to a certain value, irrespective of the displacement amplitude. The quantity of cumulative energy absorption multiplied by the yielding ratio is at the same level, regardless of the steel grade and displacement amplitude. The absolute quantity of energy absorption may be used as one means of evaluating the deformation capacity of high-strength steel beams.

ACKNOWLEDGEMENT

REFERENCES

1. E.P.Popov, et. al.; " Cyclic Loading of Steel Beams and Connections " Proc. ASCE ; No. ST 6, 1973.

2. P.F.Adams.; " Plastic Design in High-Strength Steel. " Fritz Engineering Laboratory Report. No.297, May, 1966.

3. J.Sakamoto.; " Cumulative Plastic Deformation of Framed Structure subjected to Alternating Displacement. " Trans. of AIJ, No.246, 1976.

4. T.Suzuki and T.Ono.; " An Experimental Study on Inelastic Behavior of Steel Members subjected Repeated Loading " 6-WCEE, 11-171, 1977.

5. T.Suzuki and K.Tamamatsu.; " Experimental Study on Energy Absorption Capacity of Columns of Low Steel Structures Part. 1 " Trans. of AIJ, No.279, 1979.

Table 1 Material Properties

Steel*	Thickness (mm)	σ_y (t/cm^2)	σ_u (t/cm^2)	σ_y $(\times 10^{-6})$	S. $(\varepsilon/\varepsilon_y)$
SM-41	12	3.24	4.76	1521.	13.8
SM-50	12	3.95	5.53	1855.	10.6
HT-60-1	12	5.78	6.78	2706.	6.78
HT-60-2	12	5.45	6.65	2547.	5.89
HT-80	12	8.80	9.39	4112.	1.00

Steel*	$E \times 10^3$ (t/cm^2)	Est (t/cm^2)	σ_u/σ_y	h (E/Est)	Elong. (%)
SM-41	2.13	47.0	1.47	45.3	28.5
SM-50	2.13	36.1	1.40	59.0	23.4
HT-60-1	2.14	31.0	1.17	69.0	26.6
HT-60-2	2.14	36.4	1.20	58.0	30.7
HT-80	2.14	15.0	1.07	142.7	24.4

Note : *Test Coupon Dimension (JIS Z 2201)
       SM-41,SM-50 : No.1 Test Coupon
       HT-60,HT-80 : No.5 Test Coupon

Table 2 Specimens

Specimen	Steel	L/ry	Mp (t·cm)	Vp (cm)	Amplitude
A-41-1	SM-41	49.5	1690.0	2.31	3.0Vp (6.9cm)
A-41-2	SM-41	49.5	1690.0	2.31	4.0Vp (9.2cm)
A-41-3	SM-41	49.5	1690.0	2.31	5.0Vp (11.5cm)
A-41-4	SM-41	49.5	1690.0	2.31	3.0,4.0,5.0Vp
A-60-1	HT-60-1	49.5	3015.0	4.10	2.0Vp (8.2cm)
A-60-2	HT-60-1	49.5	3015.0	4.10	2.5Vp (10.2cm)
A-60-3	HT-60-2	49.5	2842.8	·3.87	3.0Vp (11.6cm)
A-60-4	HT-60-1	49.5	3015.0	4.10	2.0,2.5,3.0Vp
A-80-1	HT-80	49.5	4590.3	6.25	1.5Vp (9.4cm)
A-80-2	HT-80	49.5	4590.3	6.25	2.0Vp (12.5cm)
A-80-3	HT-80	49.5	4590.3	6.25	1.5,2.0Vp
B-41-1	SM-41	76.1	1690.0	1.90	3.5Vp (6.7cm)
B-41-2	SM-41	76.1	1690.0	1.90	6.0Vp (11.4cm)
B-50-1	SM-50	76.1	2060.4	2.32	2.5Vp (5.8cm)
B-50-2	SM-50	76.1	2060.4	2.32	5.0Vp (11.6cm)
B-60-1	HT-60-2	76.1	2842.8	3.18	2.0Vp (6.4cm)
B-60-2	HT-60-2	76.1	2842.8	3.18	2.5Vp (8.0cm)
B-60-3	HT-60-2	76.1	2842.8	3.18	3.0Vp (9.6cm)
B-80-1	HT-80	76.1	4590.3	5.14	1.4Vp (7.2cm)
B-80-2	HT-80	76.1	4590.3	5.14	1.7Vp (8.7cm)
B-80-3	HT-80	76.1	4590.3	5.14	2.0Vp (10.2cm)

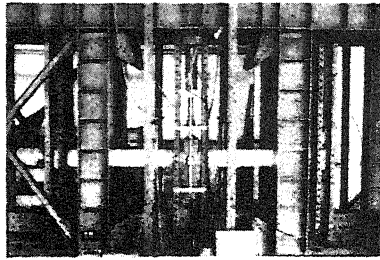Photo. 1 Test Setup

A Type

B Type

Section
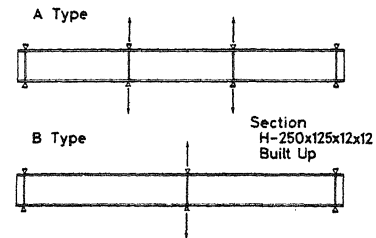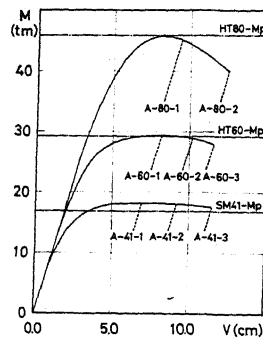H-250x125x12x12
Built Up

Fig. 1 Loading Condition

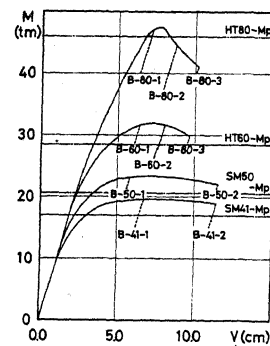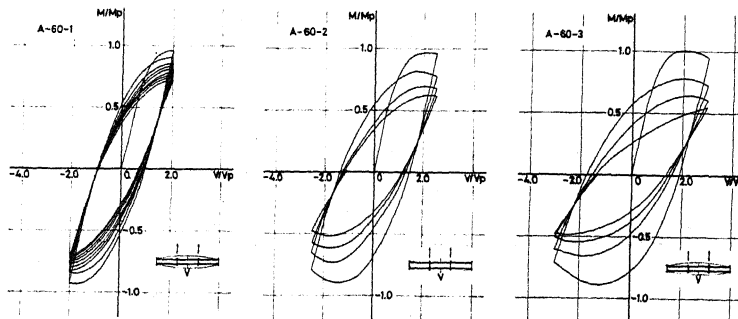Fig. 2 Repeated Displacement

Fig. 3 Repeated Displacement

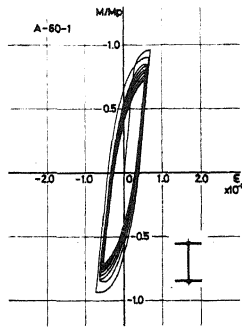Fig. 4 Hysteresis Loop　Fig. 6 Hysteresis Loop　Fig. 5 Hysteresis Loop
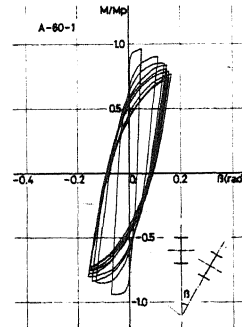
236

Fig. 7 Axial Strain
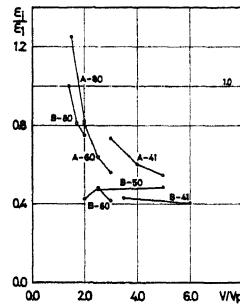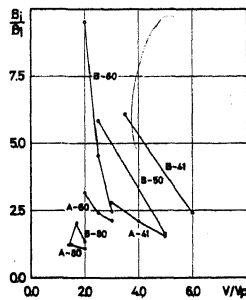

Fig. 8 Torsional Deformation

Fig. 9 Accumulated Axial Strain
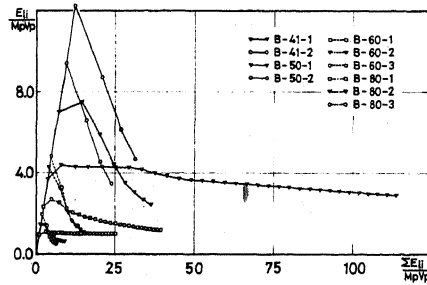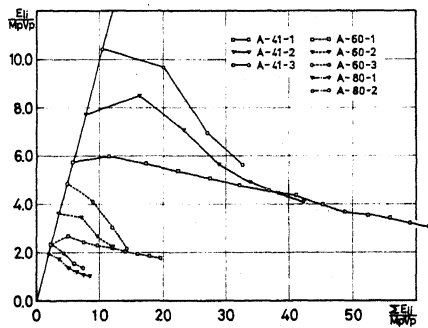

Fig. 10 Accumulated Torsional Def.

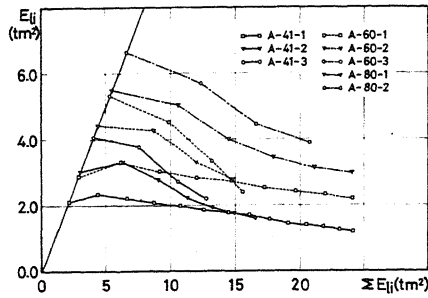Fig. 11 Accumulated Energy of A type

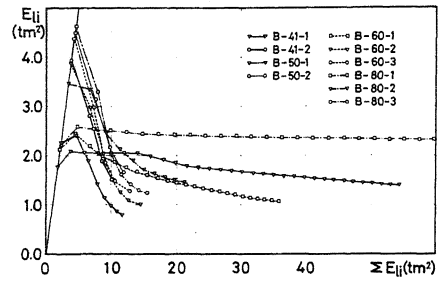Fig. 12 Accumulated Energy of B type

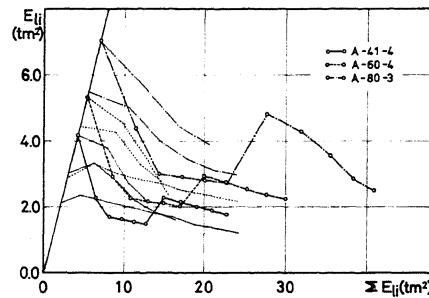Fig. 13 Accumulated Energy of A type

Fig. 14 Accumulated Energy of B type

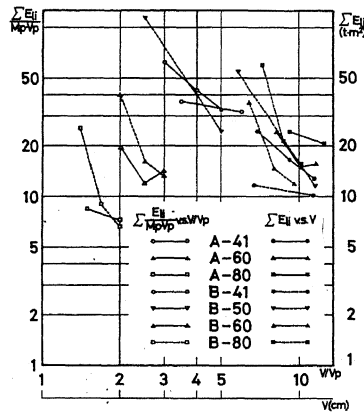Fig. 15 Accumulated Energy of
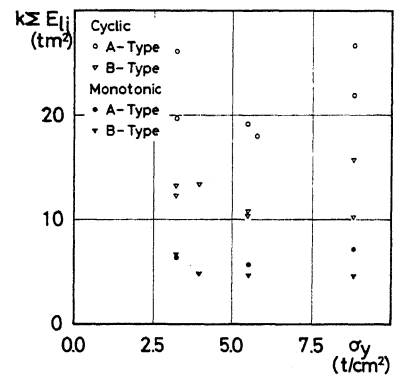Random Amplitude

Fig. 16 Accumulated Energy-Deflection

Fig. 17 Accumulated Energy
($k = \sigma_u/\sigma_y$)

238